

HIGH-GAIN LOW SIDE LOBE LEVEL FABRY PEROT CAVITY ANTENNA WITH FEED PATCH ARRAY

A. R. Vaidya^{*}, R. K. Gupta, S. K. Mishra, and J. Mukherjee

Electrical Engineering Department, Indian Institute of Technology Bombay, Mumbai-400 076, India

Abstract—In this paper, a high gain, low side lobe level Fabry Perot Cavity antenna with feed patch array is proposed. The antenna structure consists of a microstrip antenna array, which is parasitically coupled with an array of square parasitic patches fabricated on a FR4 superstrate. The patches are fabricated at the bottom of superstrate and suspended in air with the help of dielectric rods at $0.5\lambda_0$ height. Constant high gain is obtained by resonating parasitic patches at near close frequencies in 5.725–5.875 GHz ISM band. The structure with 9×9 square parasitic patches with $1.125\lambda_0$ spacing between feed elements is fabricated on $5\lambda_0 \times 5\lambda_0$ square ground. The fabricated structure provides gain of 21.5 dBi associated with side lobe level less than -25 dB, cross polarization less than -26 dB and front to back lobe ratio of more than 26 dB. The measured gain variation is less than 1 dB and VSWR is less than 2 over 5.725–5.875 GHz ISM band. The proposed structures are good candidates for base station cellular systems, satellite systems, and point-to-point links.

1. INTRODUCTION

Microstrip antenna (MSA) has distinct features such as low weight, small size, ease of fabrication, ease of integration with Microwave Integrated Circuits (MICs), which make it very popular and is widely used. However, MSA has certain drawbacks such as low gain, narrow bandwidth, low efficiency, and low power handling capability [1]. High directivity planar antenna structures for long-range wireless links such as reflectarray antennas have been proposed to overcome the low directivity of MSA [2–4]. Reflectarray structures

Received 15 March 2012, Accepted 9 April 2012, Scheduled 13 April 2012

^{*} Corresponding author: Avinash R. Vaidya (arvaidya@ee.iitb.ac.in).

can be made conformal to a surface and do not require feed line network but suffer from low efficiency due to dielectric losses. A number of gain enhancement techniques based on Fabry Perot Cavity (FPC) are reported [5–8]. In these structures, the dielectric layer is placed at approximately 0.5λ above a ground plane, which acts as a Partially Reflecting Surface (PRS). Gain of such an antenna depends on the reflection coefficient of PRS and radiation characteristics of feed element. These of structures are fed using a dipole, waveguide or MSA. High gain antennas using Artificial Magnetic Conductors (AMC) based on FPC model, Frequency Selective Surface (FSS), Electromagnetic Band Gap (EBG) resonator have also been proposed [9–13]. The analysis of antennas using the resonance gain method and Finite-Difference Time-Domain (FDTD) techniques have been studied [14, 15]. In addition, leaky wave analysis has been carried out for explaining high gain phenomenon [16]. Space fed three dimensional, efficient and directive antenna arrays using a single feed patch have been proposed, but these antennas suffer from high Side Lobe Level (SLL) for small array size [17].

Low cost, efficient antenna using an array of Parasitic Patches (PPs) has been reported in [18]. The structure is fed by MSA. It offers high efficiency but has limited gain. Microstrip Reflectarray Antenna (MRA) with Minkowski shape radiating element has been proposed in [19]. This antenna array has lower SLL of about -25 dB, but the structure suffers from design complexity. An array antenna applied to WLAN communication system has been proposed in [20], which achieves the maximum gain of 15.90 dBi (E -plane) and 15.85 dBi (H -plane) at 2480 MHz, but it suffers from high SLL. An efficient, high gain and low SLL antenna using PPs on multilayer superstrates is discussed in [23]. SLL is improved using square PP array on multilayer superstrate, but the overall structure becomes bulky because of the multilayer superstrates. In structures with PPs on superstrate layer, high gain with low SLL and low cross polarization is desirable.

However, in literature, antenna structures are fed by single antenna element despite the availability of space available near the feed antenna. Structure with PPs on superstrate layer can exhibit better radiation characteristics, if radiation parameters of the feed element are improved. Available lateral space near the feed patch can be utilized to add more radiating elements. The antenna structure can be fed by MSA array to increase performance in terms of radiation parameters.

In this paper, MSA array fed constant high gain and low SLL antenna structures using square PPs on superstrate layer are proposed for the 5.725–5.875 GHz ISM band. The antenna structures consist of a MSA Feed Patch Array (FPA) parasitically coupled with Square

Parasitic Patch Array (SPPA) fabricated on a FR4 superstrate. Instead of single Feed Patch (FP), MSA array is used as feed element and the available lateral space near the FP is utilized. The proposed structures have simple design and offer dimensional flexibility. Desired gain with low SLL can be obtained by using different PP array size. The following sections deal with the antenna geometry, design theory, simulation and measurement results.

2. ANTENNA GEOMETRY AND DESIGN THEORY

The geometry of the designed antenna structure (side view) is shown in Figure 1(a), whereas, FPA is shown in Figure 1(b). The FPA consists of a square array of patches having identical dimensions. The patches are of 0.5 mm thickness and are placed at a height $H = 2$ mm from the ground plane. The top view of 4×4 and 5×5 SPPA on a superstrate layer is shown in Figure 1(c). The PPs are fabricated at the bottom side of 1.59 mm thick low cost FR4 superstrate at height 'HS' from the FPA, which also acts as a radome to the antenna. Relative permittivity (ϵ_r) and loss tangent ($\tan \delta$) of FR4 superstrate is 4.4 and 0.02 respectively. Air is used as a dielectric medium between FPA, ground plane and superstrate layer to achieve high efficiency. FPA is fed through a coaxial probe of 50Ω . The antenna is designed to operate over 5.725–5.875 GHz ISM band. The superstrate layer is positioned at height of $0.5\lambda_0$ above ground plane, where λ_0 is the free space wavelength corresponding to central frequency 5.8 GHz. Simulations and optimizations of structures are carried out using Zeland IE3D 14.0 software [26]. IE3D is a Method-of-Moment (MOM) non-uniform meshing simulator. In simulations, highest frequency is 6 GHz and number of cells per wavelength are kept as 15.

The structure can be considered as a cavity resonator with PRS. The structure is a half wavelength FPC consisting of a ground plane and a PRS, which results in multiple reflections between ground plane and PRS. If the distance between the ground plane and PRS is kept such that it causes the waves emanating from PRS to be in phase in normal direction, a broadside directive radiation pattern can be achieved. If ' $\rho e^{j\psi}$ ' is the reflection coefficient of the PRS and ' $f(\alpha)$ ' is the normalized field pattern of feed antenna, normalized electric field ' E ' and power ' S ' at an angle ' α ' to the normal can be derived as [5]

$$|E| = \sqrt{\frac{1 - \rho^2}{1 + \rho^2 - 2\rho \cos \phi}} f(\alpha) \quad (1)$$

$$S = \frac{1 - \rho^2}{1 + \rho^2 - 2\rho \cos \phi} f^2(\alpha) \quad (2)$$

Here, ' ϕ ' is the phase difference between waves emanating from PRS. Boresight gain ($\phi = 0^\circ$ and bandwidth are function of reflection coefficient [5, 6]

$$G = (1 + \rho)/(1 - \rho) \quad (3)$$

$$\text{BW} = \Delta f/f_o = (\lambda/2\pi L_r)(1 - \rho)/\rho^{0.5} \quad (4)$$

Resonant distance ' L_r ' between ground plane and PRS is given by

$$L_r = \left(\frac{\psi_0}{360} - 0.5 \right) \frac{\lambda}{2} + N \frac{\lambda}{2} \quad (5)$$

Here ψ_0 is expressed in degree and $N = 0, 1, 2, 3$ etc..

Radiation pattern of structure with FPA can be analyzed by considering top dielectric layer as a PRS, while the structure below it as a feed antenna with field pattern $f(\alpha)$. Radiation pattern of such structures depends on two frequency sensitive processes — one is the resonant interaction of waves with metallic patches and other is the interference of waves reflected from PRS [10]. Gain of structure also depends on the reflection coefficient of PRS. Metallic patches fabricated at bottom of substrate act as good reflector of microwave frequency and therefore can be used to enhance the reflection coefficient and the gain. Gain of the antenna depends on the spacing between patches and their dimensions, as waves emanating from the PRS must be cophasal [18].

High gain phenomenon can be also explained based on increase in the effective aperture area. It is observed that, superstrate layer has a focusing effect. The phase distributions of the fields with a superstrate are observed to be more uniform than one without the superstrate leading to an increase in effective aperture area and gain. The focusing effect or phase smoothening and hence gain increases with increase in dielectric constant and thickness of superstrate [21].

When a FPA feeds SPPA, high gain broadside radiation can be achieved if the PPs are fed in phase and current induced at patches are in phase. Since the PPs are positioned at different location and at different distance from FP, therefore, feed to each element involves amplitude tapering and phase delay. Beside the amplitude tapering due to distance, there is additional amplitude tapering due to the radiation pattern of FPA. The amplitude tapering results in decrease in gain but it improves side lobe level. Hence, reasonably high gain array antenna with a desired SLL can be achieved. Feed amplitude to a PP decreases as its distance from FPA increases, therefore PPs which are located far from FPA contribute less to radiating field. The amplitude tapering increases progressively with increase in distance from FPA and differential gain improvement decreases with increase in array size on a layer. Gain of such a antenna also depends on PP dimensions and spacing and superstrate height [22].

3. ANALYSIS AND RESULTS ON INFINITE GROUND PLANE

3.1. Design and Optimization of Feed Patch Array

A metal (copper) plated MSA is designed to operate over 5.725–5.875 GHz, ISM band. Then, 2×2 MSA array with feed network is designed as shown in Figure 1(b). In the designed structure, a microstrip line corporate feed network is used. As shown in Figure 1(b), initial feed is given using a 50Ω microstrip line (a), which is connected to 100Ω microstrip lines (b) on either side. Each 100Ω microstrip

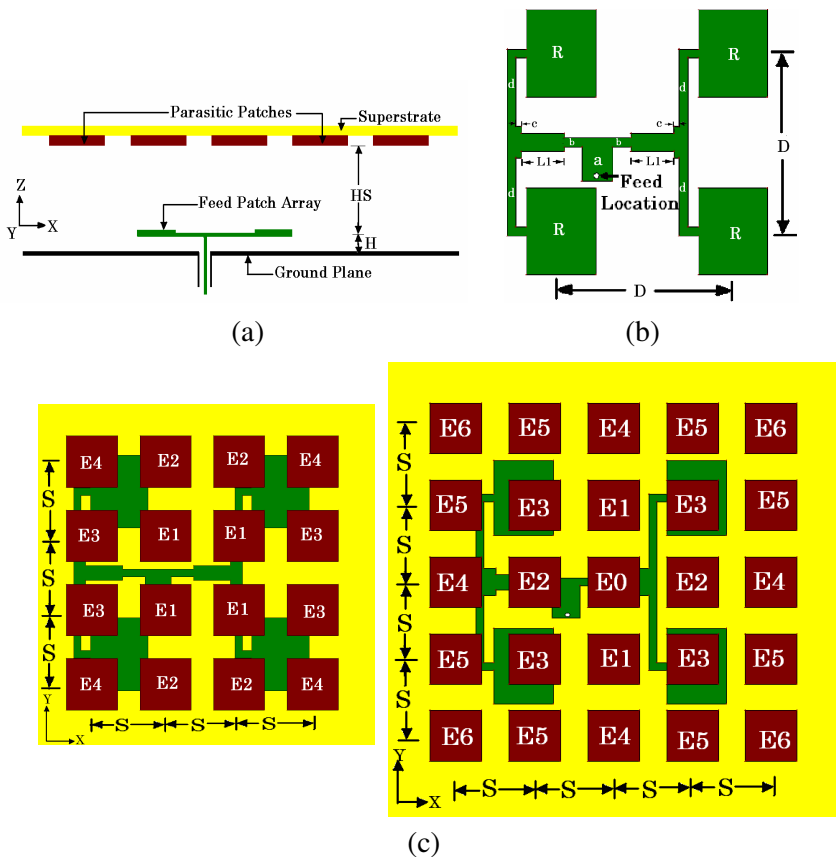


Figure 1. Geometry of proposed antenna structure. (a) Side view. (b) Top view of FPA. (c) 4×4 and 5×5 SPPA on a superstrate layer (top view).

Table 1. Radiation parameters of FPA.

FPA	Gain (dBi)	SLL (dB)	Cross Pol. (dB)
$D = \lambda_0$	12.1	-18.0	-13.0
$D = 1.125\lambda_0$	12.4	-17.7	-15.6
$D = 1.25\lambda_0$	12.0	-15.0	-14.5

feed line is matched to $50\ \Omega$ microstrip line (c) using a $70.1\ \Omega$ quarter wave transformer of length $L1 = 13\ \text{mm}$ and $50\ \Omega$ microstrip line (c) is connected to $100\ \Omega$ microstrip line (d). Each radiating element (R) is edge fed using $100\ \Omega$ microstrip transmission line (d). The length of radiating element (R) is calculated using equations in [24] as,

$$L_{eff} = L + 2\Delta L \quad (6)$$

Here ' L_{eff} ' is the total length of radiating element, where, value of ' ΔL ' is given as,

$$\frac{\Delta L}{h} = 0.412 \frac{(\varepsilon_{reff} + 0.3) \left(\frac{W}{h} + 0.264\right)}{(\varepsilon_{reff} - 0.258) \left(\frac{W}{h} + 0.8\right)} \quad (7)$$

where, ' L ' and ' ΔL ' are length and extended length of the radiating element respectively.

The MSA provides a gain of 9.4 dB and 2×2 MSA array with feed network referred as FPA placed at height $H = 2\ \text{mm}$, provides gain of 12.1 dBi. If the distance ' D ' between feed elements is more than λ_0 , grating lobes are observed in radiation pattern [24]. Distance between array elements can be increased avoiding grating lobes and cross polarization, if superstrate is placed above FPA [25]. As the distance between array elements is varied from $1.0\lambda_0$ to $1.25\lambda_0$, the maximum gain is obtained at $D = 1.125\lambda_0$. Gain, SLL and cross polarization of 2×2 feed patch array for different ' D ' are tabulated in Table 1, while impedance variation plots are shown in Figure 2.

3.2. Parasitic Patch Array on Superstrate Layer

When a superstrate layer is placed above FPA at a height of $0.5\lambda_0$ from ground plane, gain increases to 14.1 dBi with $-15\ \text{dB}$ SLL. Thereafter a single square parasitic patch, E0 is placed at the bottom of a FR4 and its dimensions are optimized to achieve maximum gain. Then square PPs are placed at the bottom of a superstrate layer to form an even and odd array as shown in Figure 1(c).

Optimization of SPPA structure is carried by placing the PPs from inner to outer and structure is optimized at each step to achieve

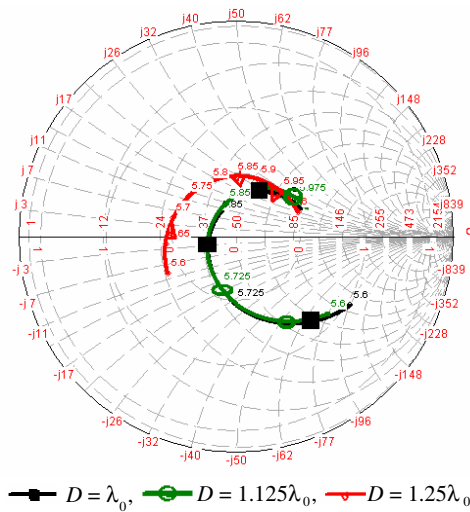


Figure 2. Impedance variation of FPA.

maximum gain. In 4×4 SPPA as shown in Figure 1(c), four elements ‘E1’ are placed at the bottom of FR4 superstrate to form 2×2 SPPA. Thereafter, elements ‘E2’ and ‘E3’ are placed at sides of element ‘E1’ and four corner elements ‘E4’ are placed which forms 4×4 SPPA. Dimensions are optimized to achieve desired radiation performance. Similar process is followed to form higher order even SPPAs and structures are optimized. Dimensions of PPs are optimized to resonate in 5.725–5.875 GHz band, to achieve constant high gain and directive radiation pattern over the operating 5.725–5.875 GHz frequency band ISM band. Optimized dimension of each PP is $17 \times 17 \text{ mm}^2$. PPs with identical size resonate at different near frequencies in 5.725–5.875 GHz band as they are located at different distance from FPA resulting in constant high gain. Simultaneously, structures are also optimized for inter-element spacing, ‘S’. PP is also fed from nearby patches, which must be in phase to obtain high gain. The maximum gain is obtained with inter element spacing, ‘S’ = 1.0λ , where λ is wavelength in dielectric corresponding to central frequency 5.8 GHz. Similarly, in 5×5 SPPA shown in Figure 1(c), first the centre element ‘E0’ is placed at the bottom of FR4 superstrate. The structure with only ‘E0’ element is referred as 1×1 SPPA. Then, element ‘E1’ is placed on both sides of ‘E0’ at an inter element spacing ‘S’ and its dimensions are optimized to achieve maximum gain. Thereafter element ‘E2’ is placed on both sides and corner elements ‘E3’ are placed and optimized which forms 3×3 SPPA. Elements ‘E4’ are placed on sides of ‘E1’ and ‘E2’ and

then corner elements ‘E5’ and ‘E6’ are placed at four corners to form 5×5 array and optimized. Similar process is followed to form higher order odd SPPAs and structures are optimized for desired radiation characteristics. Similar to even size SPPAs, inter-element spacing ‘S’ is also optimized. Each element in SPPA is of size $17 \times 17 \text{ mm}^2$ and ‘S’ is 1.0λ .

Structures with 1×1 to 9×9 SPPA are optimized at superstrate height $HS = 0.5\lambda_0$. It is observed that gain increases with increase in size of SPPA. Feed amplitude to a PP decreases as its distance from FPA increases, therefore, PPs which are located far from FPA contribute less to radiating field, as a result, though, gain increases

Table 2. Radiation parameters of constant high gain antennas with FPA on infinite ground at 5.8 GHz.

Structure (SPPA)	Gain (dBi)	SLL (dB)
	$D = \lambda_0, 1.125\lambda_0, 1.25\lambda_0$	$D = \lambda_0, 1.125\lambda_0, 1.25\lambda_0$
Superstrate	14.1, 15.3, 15.0	-15.0, -13.0, -10.0
1×1	14.5, 16.0, 15.8	-15.5, -10.2, -10.3
2×2	16.4, 17.2, 16.8	-15.6, -15.0, -12.3
3×3	17.8, 18.0, 16.9	-19.3, -16.2, -12.6
4×4	18.2, 18.3, 18.0	-18.6, -18.5, -15.2
5×5	18.7, 19.3, 19.0	-22.0, -20.0, -15.5
6×6	19.4, 20.0, 19.5	-20.5, -21.3, -18.0
7×7	20.1, 20.3, 19.7	-25.0, -23.0, -21.3
8×8	20.4, 20.6, 20.0	-20.0, -23.0, -21.7
9×9	20.6, 21.1, 20.4	-22.5, -25.0, -23.0
Structure (SPPA)	Cross Pol. (dB)	-
	$D = \lambda_0, 1.125\lambda_0, 1.25\lambda_0$	-
Superstrate	-23.5, -20.0, -20.0	-
1×1	-23.3, -20.3, -21.0	-
2×2	-26.5, -23.2, -19.0	-
3×3	-26.5, -23.1, -18.0	-
4×4	-24.9, -23.8, -20.0	-
5×5	-27.5, -25.1, -19.3	-
6×6	-26.5, -26.0, -21.3	-
7×7	-25.0, -25.6, -23.3	-
8×8	-26.2, -23.0, -23.3	-
9×9	-25.2, -26.0, -23.8	-

with increase in size of SPPA, but differential gain improvement decreases with increase in size of array on a superstrate layer. Radiation parameters of structures for FPA with $D = \lambda_0$, $D = 1.125\lambda_0$ and $D = 1.25\lambda_0$ on infinite ground at 5.8 GHz are tabulated in Table 2.

FPA with $D = \lambda_0$ and 9×9 SPPA provides a gain of 20.6 dBi with more than 90% antenna efficiency and SLL of -22.5 dB and cross

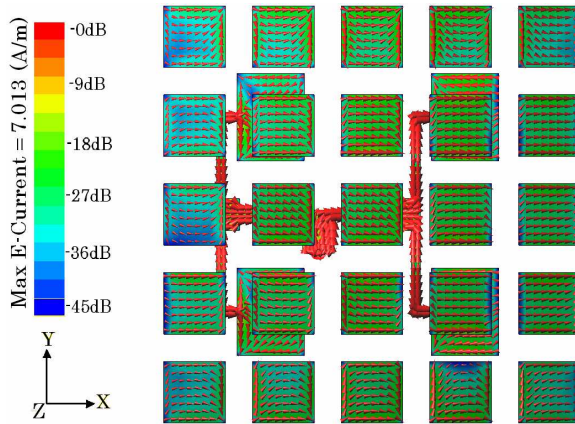


Figure 3. Current distribution of FPA ($D = 1.125\lambda_0$) with 5×5 SPPA at 5.8 GHz.

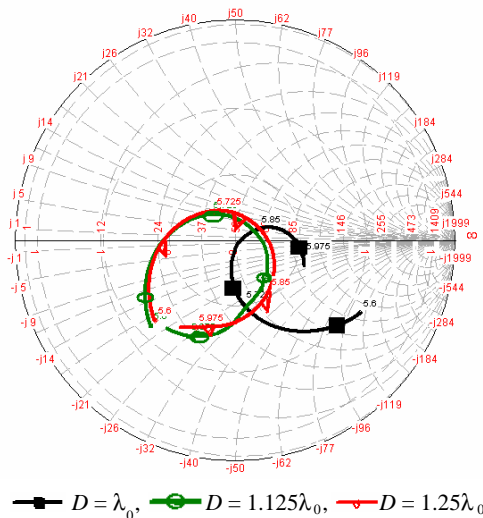


Figure 4. Impedance variation of FPAs with 9×9 SPPA.

polarization of -25.2 dB. Also, FPA with $D = 1.125\lambda_0$ and 9×9 SPPA provides a gain of 21.1 dBi with more than 95% antenna efficiency and SLL of -25.0 dB and cross polarization of -26.0 dB. FPA with $D = 1.25\lambda_0$ and 9×9 SPPA provides a gain of 20.4 dBi with more than 90% antenna efficiency and SLL of -23.0 dB and cross polarization of -23.8 dB. Gain variation for all structures is less than 1 dB over 5.725 – 5.875 GHz ISM band. Structures with different SPPAs at $HS = 0.5\lambda_0$ provide gain ranging from 14.1 – 21.1 dB and SLL improves significantly in larger size SPPAs.

Figure 3 shows average and vector current distribution at the FPA and PPs in 5×5 SPPA at 5.8 GHz. The current induced in PPs is nearly in phase and decreases as its distance from FPA increases. From Figure 3, it can be observed that, both FPA and PPs contribute to radiating fields. The superstrate also affects the phase and amplitude distribution of fields [18]. Impedance variation of FPAs with 9×9 SPPA is shown in Figure 4. Radiation patterns of FPAs with 9×9 SPPA on infinite ground at 5.8 GHz are shown in Figure 5. Radiation patterns are directive with low SLL and cross polarization.

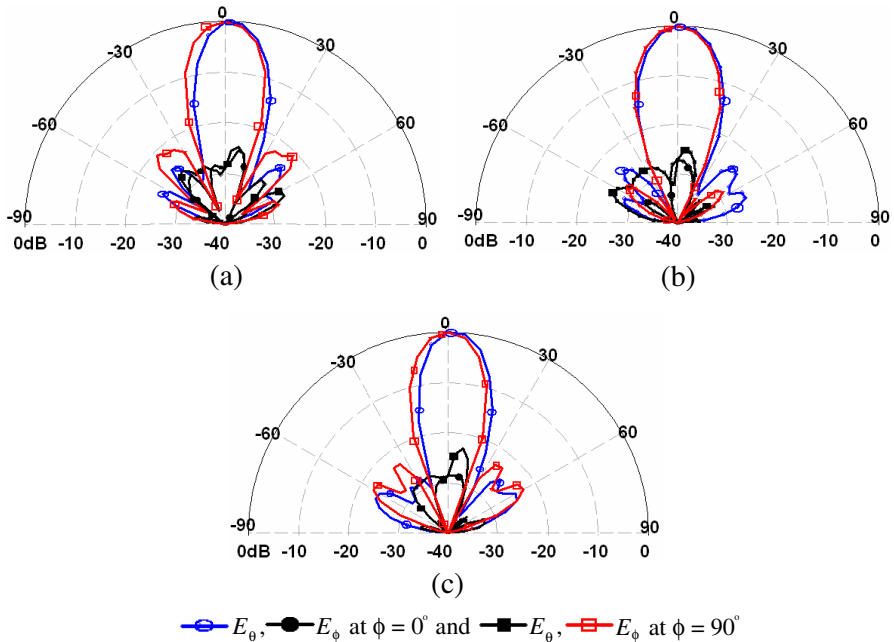


Figure 5. Radiation patterns of 9×9 SPPA antenna at 5.8 GHz on infinite ground plane. (a) $D = \lambda_0$. (b) $D = 1.125\lambda_0$. (c) $D = 1.25\lambda_0$.

Table 3. Radiation parameters of FPA fed constant high gain antennas on finite ground at 5.8 GHz.

Structure	Gain (dBi)	SLL (dB)	F/B (dB)	Cross Pol. (dB)	Ground Plane size
9×9 ($D = \lambda_0$)	20.7	-26.0	27.0	-24.5	$5\lambda_0 \times 5\lambda_0$
9×9 ($D = 1.125\lambda_0$)	21.2	-26.0	26.0	-25.0	$5\lambda_0 \times 5\lambda_0$
9×9 ($D = 1.25\lambda_0$)	20.6	-25.0	27.0	-26.0	$5\lambda_0 \times 5\lambda_0$

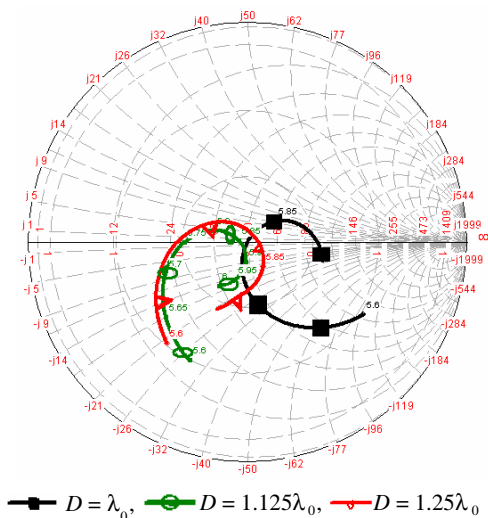


Figure 6. Impedance variation on finite ground of 9×9 SPPA.

4. ANTENNA REALIZATION ON FINITE GROUND, FABRICATION AND MEASUREMENT RESULTS

The FPA with 9×9 SPPA structures are redesigned on finite ground plane of size $5\lambda_0 \times 5\lambda_0$. Radiation parameters viz. gain, SLL, front to back lobe (F/B) ratio and cross polarization of these structures are tabulated in Table 3. Constant high gain is obtained in 5.725–5.875 GHz ISM band. It is observed that in some structures gain increases slightly with finite ground. This is attributed to constructive interference between radiated and reflected waves at particular dimensions of finite ground. Plots for impedance variation vs. frequency are shown in Figure 6 and VSWR vs. frequency plots are shown in Figure 7. Antenna efficiency vs. frequency plots are shown in Figure 8.

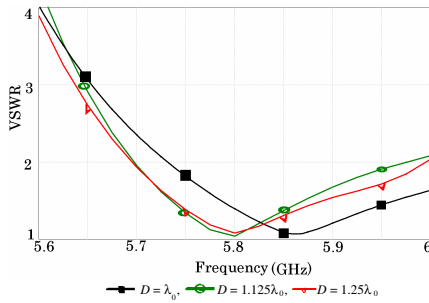


Figure 7. VSWR vs. frequency of 9×9 SPPA.

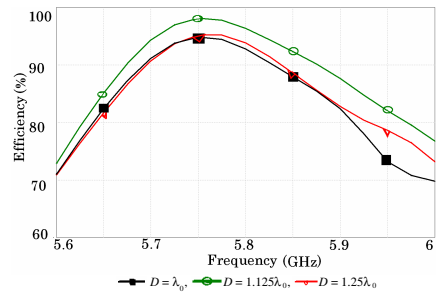
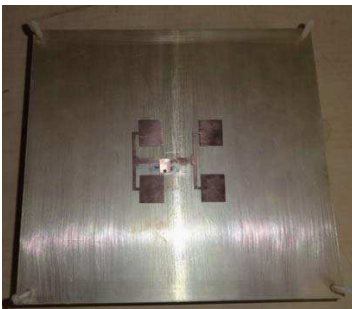
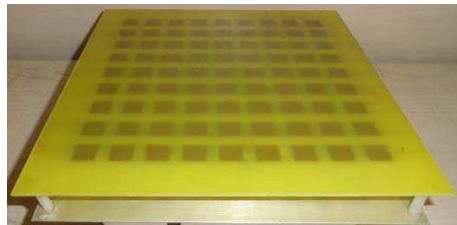


Figure 8. Antenna efficiency vs. frequency of 9×9 SPPA on finite ground.



(a)



(b)

Figure 9. Fabricated structure. (a) Fabricated feed patch array with $D = 1.125\lambda_0$. (b) Fabricated structure of FPA ($D = 1.125\lambda_0$) with 9×9 SPPA.

FPA ($D = 1.125\lambda_0$) with 9×9 SPPA antenna structure is most efficient in terms of gain and radiation characteristics as shown in Table 3, hence it is fabricated and tested. Fabricated structure is shown in Figure 9. VSWR measurement is performed using Agilent VNA (8722ET). Measured and simulated VSWR plots for this structure are shown in Figure 10. Radiation pattern and gain are measured using standard horn antennas. Radiation pattern measurement is performed using Compact Antenna Radiation (CAR) measurement setup. Measured and simulated gain variations on finite ground are shown in Figure 11. The gain variation over the frequency range 5.725–5.875 GHz is found to be less than 1 dB with maximum gain of 21.5 dBi at 5.8 GHz. Figure 12 shows measured radiation patterns at 5.8 GHz

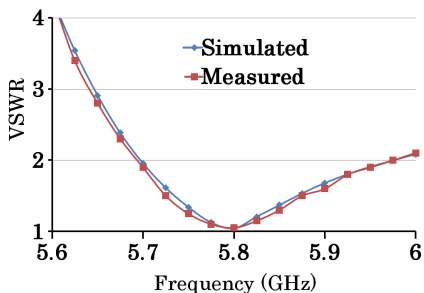


Figure 10. VSWR vs. frequency of FPA ($D = 1.125\lambda_0$) with 9×9 SPPA.

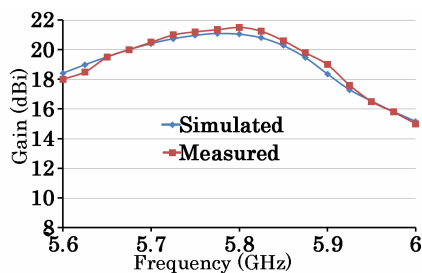


Figure 11. Gain vs. frequency of FPA ($D = 1.125\lambda_0$) with 9×9 SPPA.

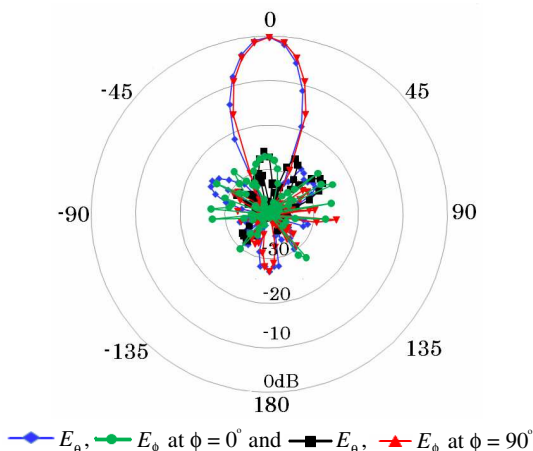


Figure 12. Measured radiation patterns of FPA ($D = 1.125\lambda_0$) with 9×9 SPPA antenna at 5.8 GHz.

for fabricated structure. SLL is less than -26 dB and F/B ratio is about 26 dB with less than -25 dB cross polarization.

5. CONCLUSION

High gain, low side lobe level antenna with feed patch array and parasitic patch array on a superstrate layer is proposed for wireless application. The antenna is designed using low cost easily available FR4 superstrate and copper plates. The structure provides design flexibility as the desired gain can be obtained by using different

square parasitic patch arrays. The structure provides uniform gain with less than 1 dB gain variation over the frequency range 5.725–5.875 GHz. Differential gain improvement decreases with increase in size of array on superstrate. Proposed FPA ($D = 1.125\lambda_0$) with 9×9 SPPA antenna structure provides 21.5 dBi gain with SLL less than -25 dB, cross polarization less than -26 dB and F/B ratio more 26 dB. Impedance bandwidth and radiation pattern characteristics over 5.725–5.875 ISM band clearly indicate that the proposed antenna is capable of generating efficient directive radiation pattern in the desired frequency band.

ACKNOWLEDGMENT

The authors thank to Mr. V. Srinivas Rao, Scientist, RCI, DRDO, Hyderabad, INDIA for providing measurement facilities. This work is supported in part by the Department of Science and Technology (DST), Government of India.

REFERENCES

1. Kumar, G. and K. P. Ray, *Broadband Microstrip Antennas*, Artech house, Norwood, MA, 2003.
2. Pozar, D. M., S. D. Targonski, and H. Syrigos, "Design of millimeter wave microstrip reflectarrays," *IEEE Trans. Antennas Propagat.*, Vol. 45, No. 2, 287–295, Feb. 1997.
3. Javor, R. D., X. D. Wu, and K. Chang, "Design and performance of a microstrip reflectarray antenna," *IEEE Trans. Antennas Propagat.*, Vol. 43, No. 9, 932–939, Sep. 1995.
4. Vazquez Antuna, C., G. R. Hotopan, S. Ver Hoeye, M. Fernandez Garcia, L. F. Herran Ontanon, and F. Las-Heras, "Microstrip antenna design based on stacked patches for reconfigurable two dimensional planar array topologies," *Progress In Electromagnetics Research*, Vol. 97, 95–104, 2009.
5. Trentini, G. V., "Partially reflecting sheet arrays," *IEEE Trans. Antennas Propagat.*, Vol. 4, 666–671, Oct. 1956.
6. Feresidis, A. P. and J. C. Vardaxoglou, "High gain planar antenna using optimized partially reflective surfaces," *IEE Proc. Microw. Antennas Propagat.*, Vol. 148, 345–350, 2001.
7. Kaklamani, D. I., "Full-wave analysis of a Fabry-Parot type resonator," *Progress In Electromagnetics Research*, Vol. 24, 279–310, 1999.

8. Costa, F. and A. Monorchio, "Design of subwavelength tunable and steerable Fabry-Parot/leaky wave antennas," *Progress In Electromagnetics Research*, Vol. 111, 467–481, 2011.
9. Wang, S. H., A. P. Feresidis, G. Goussetis, and J. C. Vardaxoglou, "Low-profile resonant cavity antenna with artificial magnetic conductor ground plane," *Electron. Lett.*, Vol. 40, No. 7, 405–406, Jul. 2004.
10. Parker, E. A., "The gentleman's guide to frequency selective surfaces," *17th Q.M.W. Antenna Symposium*, London, Apr. 1991.
11. Boutayeb, H., A.-C. Tarot, and K. Mahdjoubi, "Focusing characteristics of a metallic cylindrical electromagnetic band gap structure with defects," *Progress In Electromagnetics Research*, Vol. 66, 89–103, 2006.
12. Pirhadi, A., F. Keshmiri, M. Hakkak, and M. Tayarani, "Analysis and design of dual band high directive EBG resonator antenna using square loop FSS as superstrate layer," *Progress In Electromagnetics Research*, Vol. 70, 1–20, 2007.
13. Ziolkowski, R. W., "FDTD simulations of reconfigurable electromagnetic band gap structures for millimeter wave applications," *Progress In Electromagnetics Research*, Vol. 41, 159–183, 2003.
14. Liu, Z.-F., P.-S. Kooi, L.-W. Li, M.-S. Leong, and T.-S. Yeo, "A method of moments analysis of a microstrip phased array in three-layered structures," *Progress In Electromagnetics Research*, Vol. 31, 155–179, 2001.
15. Yang, S., Y. Chen, and Z.-P. Nie, "Simulation of time modulated linear antenna arrays using the FDTD method," *Progress In Electromagnetics Research*, Vol. 98, 175–190, 2009.
16. Jackson, D. R. and A. A. Oliner, "A leaky-wave analysis of the high-gain printed antenna configuration," *IEEE Trans. Antennas Propagat.*, Vol. 36, No. 7, 905–910, Jul. 1988.
17. Chine, P. N. and G. Kumar, "Three dimensional, efficient, directive microstrip antenna arrays," *IEEE Int. Symposium Antennas and Propagation*, Washington DC, Jul. 2005.
18. Gupta, R. K. and J. Mukherjee, "Low cost efficient high gain antenna using array of parasitic patches on a superstrate layer," *Microwave Opt. Technol. Lett.*, Vol. 51, No. 3, 733–739, Mar. 2009.
19. Zubir, F., M. K. A. Rahim, O. B. Ayop, and H. A. Majid, "Design and analysis of a microstrip reflectarray antenna with Minkowski shape radiating element," *Progress In Electromagnetics Research B*, Vol. 24, 317–331, 2010.

20. Li, J., X. Zhao, and L. Jiang, "A novel array antenna for WLAN application," *Microwave Opt. Technol. Lett.*, Vol. 52, No. 7, 1461–1463, Jul. 2010.
21. Shen, X. H. and G. A. E. Vandenbosch, "Aperture field analysis of gain enhancement method of microstrip antennas," *IEE Int. Conf. Antenna Propagat.*, Montreal, Canada, 1997.
22. Vaidya, A. R., R. K. Gupta, S. K. Mishra, and J. Mukherjee, "Effect of superstrate height on gain of MSA fed Fabry Perot Cavity antenna," *IEEE Antennas and Propagation Conference, LAPC*, 1–4, Nov. 14–15, 2011.
23. Vaidya, A. R., R. K. Gupta, S. K. Mishra, and J. Mukherjee, "Efficient, high gain with low side lobe level antenna structures using parasitic patches on multilayer superstrate," *Microwave and Optical Technology Letters*, Vol. 54, No. 6, 1488–1493, Jun. 2012.
24. Balanis, C. A., *Antenna Theory, Analysis and Design*, John Wiley & Sons, New York, 1997.
25. Gardelli, R., M. Albani, and F. Capolino, "Array thinning by using antennas in a Fabry-Perot Cavity for gain enhancement," *IEEE Trans. Antennas Propagat.*, Vol. 54, 1979–1990, 2006.
26. IE3D release 14.0, Zeland software Inc., Fremont, CA, USA, 2008.